



## Proceedings of Science and Mathematics

Faculty of Science,  
Universiti Teknologi Malaysia

Volume 33, 2026, page 34-41

### Investigation of the Thermal Properties of Kapton-Cobalt Oxide Composite Films Under Varying Immersion Time

Lim Leng Chen<sup>a</sup>, Najaa Mustafa<sup>a\*</sup>

<sup>a</sup>Department of Chemistry, Faculty of Science, Universiti Teknologi Malaysia, 81310 UTM Skudai, Johor, Malaysia

\*Corresponding author: najaa@utm.my

#### Abstract

Kapton, a polyimide known for its high thermal stability up to 400 °C which is widely used in industries requiring high thermal performance. However, Kapton also exhibits insulating properties, which restrict its use in applications requiring both thermal and electrical conductivity. To address this limitation, Kapton can be modified by incorporating a layer of cobalt oxide on its surface using an ion-exchange method, aiming to improve its conductivity. However, not all modifications bring purely positive effects, it may compromise the material's inherent thermal stability. Immersion time of Kapton into cobalt ion solution is a factor affecting the doping efficiency which may influence the final properties of the composite film. This research focused on understanding the trade-off between improved conductivity and changes in thermal properties of Kapton-cobalt oxide (PI/Co<sub>3</sub>O<sub>4</sub>) composite films formed under varying immersion times of 30, 60 and 120 minutes. The films were characterized through ATR-FTIR and XRD. Thermal behaviour was evaluated using TGA and DSC. The formation of Co<sub>3</sub>O<sub>4</sub> on the surface of Kapton was successfully confirmed through the identification of functional groups using ATR-FTIR, which showed the Co-O bonding at 660 cm<sup>-1</sup>, and XRD which identified the (311) crystal peaks, a key indicator of Co<sub>3</sub>O<sub>4</sub> crystallization. TGA revealed that T<sub>10</sub> of PI/Co<sub>3</sub>O<sub>4</sub> is at 480 °C which is lower than T<sub>10</sub> of pure Kapton at 680 °C, suggesting that the thermal stability of PI/Co<sub>3</sub>O<sub>4</sub> is decreased due to Co<sub>3</sub>O<sub>4</sub>'s catalytic effect which accelerates the polymer's thermal degradation. DSC analysis revealed that the incorporation of Co<sub>3</sub>O<sub>4</sub> into the Kapton matrix increased the glass transition temperature (T<sub>g</sub>) due to restricted polymer chain mobility. All research objectives are successfully achieved where the formation of Co<sub>3</sub>O<sub>4</sub> is confirmed, and the thermal stability of composite films is found to be decreased as compared to pure Kapton. Under the current experimental settings, the 30-minute immersion time is identified as optimal, as it exhibited the sharpest crystalline peaks in XRD and the highest residual mass in TGA among these three conditions and showed a higher T<sub>g</sub> than pure Kapton.

**Keywords:** Kapton composite, Cobalt oxide, Thermal properties, Ion-exchange method

#### Introduction

Kapton is a polyimide material known for its exceptional thermal stability, capable of withstanding extreme temperatures up to 400 °C (Dupont, 2012). It is widely used in industries such as aerospace, electronics, and insulation, where high-performance materials are essential. Due to its unique properties, Kapton is often employed in environments that experience both low and high temperatures, ranging from -269 °C to 400 °C (Dupont, 2012). Despite these remarkable characteristics, Kapton also has insulating properties, which significantly limit its use in applications where both thermal stability and electrical conductivity are required.

This research is inspired by the need to address Kapton's limitations. Previously, researchers have explored doping Kapton with metal ions, particularly using transition metal oxides, due to their excellent thermal stability, electrical conductivity and catalytic properties (Kim et al., 2021). Among these, cobalt oxide stands out as a result of its superior electrochemical performance, thermal resilience

and environmental stability compared to other transition metal oxides (Lakra et al., 2021).  $\text{Co}_3\text{O}_4$  is preferred in the formation of oxide layer after doping as it has superior stability and functionality compared to  $\text{CoO}$ .  $\text{Co}_3\text{O}_4$  has a stable spinel structure which is more resistant to high temperatures than  $\text{CoO}$  making it ideal for applications where consistent performance under thermal stress is essential (Miranda-López et al., 2020).

One of the cost-effective methods for doping metal ions onto polymer film is the ion-exchange technique which is advantageous due to its simplicity and efficiency (Jacobs et al., 2022). In this technique, the immersion time of the substrate film in metal salts solutions becomes one of a key parameter to ensure effective metal doping (Ratnayake et al., 2021).

The significance of this study lies in its potential to enhance the functionality of Kapton for high-performance industrial applications that require both thermal stability and electrical conductivity. If the electrical conductivity of Kapton can be enhanced while maintaining its high thermal stability, this study can lead to innovations in material science and widen the use of Kapton in industries.

## Materials and methods

### 3.1. Experimental Design

The research was conducted in two main stages, the preparation and characterization of Kapton-cobalt oxide ( $\text{Co}_3\text{O}_4$ ) composite films as illustrated in Figure 1.

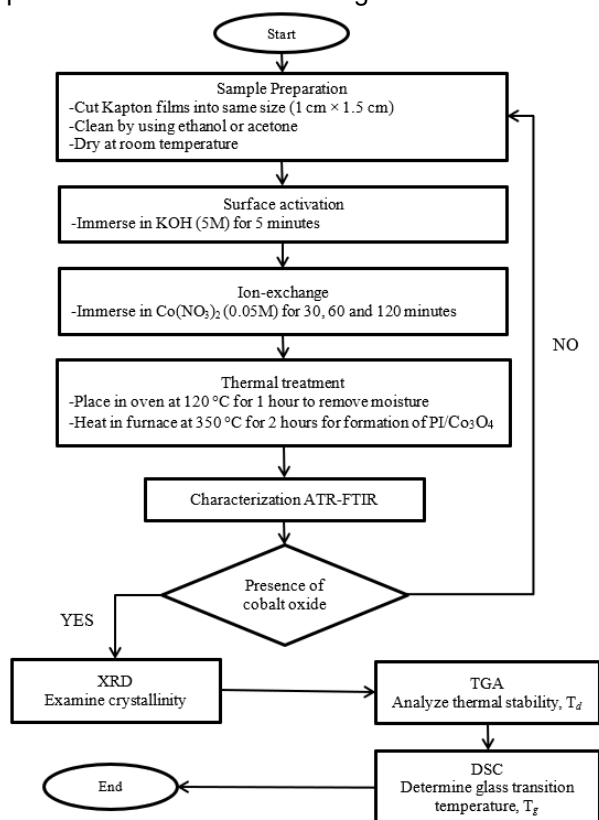


Figure 1 Experimental flowchart

### 3.2. Preparation of Kapton-Cobalt Oxide ( $\text{Co}_3\text{O}_4$ ) Composite via Ion-exchange technique

To prepare a cobalt (II) nitrate solution, cobalt (II) nitrate hexahydrate ( $\text{Co}(\text{NO}_3)_2 \cdot 6\text{H}_2\text{O}$ ) was used. The salt readily dissolved in water to produce cobalt ions ( $\text{Co}^{2+}$ ), nitrate ions ( $\text{NO}_3^-$ ) and water of hydration,  $\text{H}_2\text{O}$ . 145.52 g of cobalt (II) nitrate hexahydrate ( $\text{Co}(\text{NO}_3)_2 \cdot 6\text{H}_2\text{O}$ ) was slowly dissolved in 1L of distilled water to obtain 0.5 M cobalt (II) nitrate.

For the experimental procedure, hydrolysed Kapton films were immersed in the prepared 0.5M cobalt (II) nitrate solution for varying durations of 30 minutes, 60 minutes, and 120 minutes. After each immersion, the films were thoroughly rinsed with distilled water to remove any unreacted cobalt (II) nitrate.

Formation of cobalt oxide ( $\text{Co}_3\text{O}_4$ ) on the surface of Kapton occurred during the thermal

treatment process. The procedure began by drying the cobalt-doped films to remove residual water. Heating was performed in two stages. Initially, the film was heated from room temperature to 135 °C over 1 hour to eliminate moisture. The temperature was then gradually increased to 350 °C at a controlled rate of 2 °C per minute over 2 hours. After reaching 350 °C, the films were allowed to cool slowly inside the tubular furnace to minimize thermal stress and preserve the structural integrity of the material.

### *3.3. Characterization of Kapton-Cobalt Oxide (Co<sub>3</sub>O<sub>4</sub>) Composite Films*

The synthesized Kapton-cobalt oxide (Co<sub>3</sub>O<sub>4</sub>) Composite films were characterized using multiple techniques to evaluate their structural, chemical and thermal properties. Film thickness measurement was conducted to analyze dimensional changes resulting from cobalt doping. Attenuated total reflectance-Fourier transform infrared spectroscopy (ATR-FTIR) confirmed the presence of cobalt oxide by identifying the functional groups in undoped and doped Kapton films ensuring the doping process is successful. X-ray diffraction (XRD) analysis investigated the crystallinity and phase composition of the composite providing insights into the structural characteristics of the cobalt oxide layer. Thermogravimetric analysis (TGA) and Differential scanning calorimetry (DSC) were used to access the thermal stability, decomposition behavior and phase transitions of samples at different temperatures. As a result, these techniques were expected to provide understanding of the material's properties and behavior before and after modification.

#### *3.3.1 Film Thickness Measurement*

The thickness of the films was measured after thermal treatment to evaluate changes resulting from cobalt doping. Measurements were taken using a vernier caliper to ensure precision. Multiple measurements were recorded at different points on the films to confirm uniformity across the surface. The thickness of cobalt-doped films was compared with that of undoped Kapton films to observe the physical impact of cobalt doping on the film structure.

#### *3.3.2 Attenuated Total Reflectance-Fourier Transform Infrared Spectroscopy (ATR-FTIR)*

ATR-FTIR spectroscopy was performed to observe chemical changes and confirm the formation of cobalt oxide (Co<sub>3</sub>O<sub>4</sub>) on the surface of Kapton films. The analysis identified the functional groups present in the synthesized material helping to validate the success of the doping process. ATR-FTIR spectra were obtained using a Perkin Elmer Frontier FT-IR spectrometer equipped with a diamond attenuated total reflectance (ATR) accessory which was ideal for measurement of inorganic material. The vibrational modes were analyzed within the range of 4000 cm<sup>-1</sup> to 650 cm<sup>-1</sup>. Baseline correction was applied to improve the accuracy of results. The method ensured precise identification of chemical changes and the presence of cobalt oxide on the Kapton film surface.

#### *3.3.3 X-Ray Diffraction (XRD)*

XRD analysis examined the crystalline structure and phase composition of cobalt oxide (Co<sub>3</sub>O<sub>4</sub>) on Kapton films. This technique provided detailed insights into the crystallinity and phase identity of the synthesized composite material. The analysis utilized a Rigaku SmartLab X-ray diffractometer equipped with a Cu K $\alpha$  radiation source ( $\lambda = 1.5406 \text{ \AA}$ ). Data were collected over scattering angles ( $2\theta$ ) ranging from 2° to 80° at room temperature. The key diffraction peaks associated with cobalt oxide phases were analyzed to confirm the structural characteristics of the composite films.

#### *3.3.4 Thermogravimetric Analysis (TGA)*

TGA measured how a material's weight change as temperature increases providing insights into the decomposition behavior and thermal durability. TGA was performed using a SHIMADZU DTG-60H analyzer under an inert nitrogen atmosphere. The analysis involved two heating cycles. The first heating cycle removed moisture and residual solvents. The second cycle was conducted from room temperature to 900 °C at a heating rate of 10 °C/min. This stage was used to determine the decomposition temperature of the polymer as an assessment of its thermal stability and degradation characteristics.

### 3.3.5 Differential Scanning Calorimetry (DSC)

DSC measured heat flows associated with phase transitions. For Kapton-cobalt oxide ( $\text{Co}_3\text{O}_4$ ) composite films, DSC aimed to determine thermal stability, identify transition temperatures, and analyze phase transitions such as melting and glass transition. DSC measurement was performed using a TA Instruments Discovery DSC 25 Thermal Analyzer at a heating rate of  $10\text{ }^\circ\text{C}/\text{min}$  in a nitrogen atmosphere. Two heating cycles were employed. The first heating cycle, conducted from  $30\text{ }^\circ\text{C}$  to  $120\text{ }^\circ\text{C}$  eliminated absorbed moisture and residual solvents. After cooling the sample to room temperature, the second heating cycle increased the temperature up to  $400\text{ }^\circ\text{C}$ . This cycle identified the transition temperatures associated with specific phases in the polymer, providing a comprehensive understanding of its thermal properties.

## Results and discussion

### 4.1. Physical appearance of Kapton-Cobalt Oxide Composite Film

Upon immersion in cobalt nitrate solution, the Kapton films undergo observable physical changes. The most apparent is a darkening in color due to the surface deposition of cobalt oxide. However, this change is not significantly different among the samples immersed for 30, 60 and 120 minutes as shown in Figure 2. Darker color of the Kapton-cobalt oxide composite films is observed due to the formation of  $\text{Co}_3\text{O}_4$  which having a characteristic black appearance, indicating the successful deposition of the metal oxide on the Kapton surface.

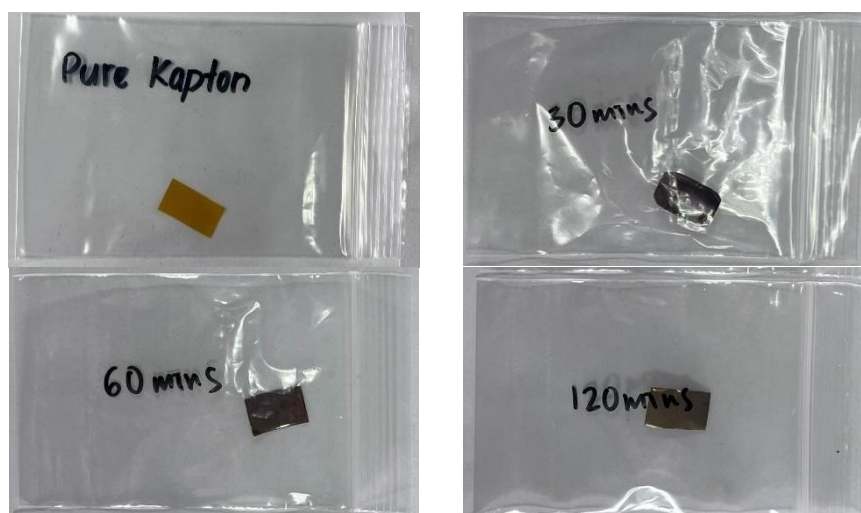


**Figure 2** Kapton-cobalt oxide composite films produced after immersion time of 30, 60 and 120 minutes

Another measurable alteration is the change in film thickness, attributed to the formation of the cobalt oxide layer. The thickness of the original Kapton film is ( $31\text{ }\mu\text{m} = 0.031\text{ mm}$ ). After 30 minutes of cobalt doping and thermal treatment, the film thickness is observed to have slightly decreased. This observation is consistent with findings by (Mu et al., 2010), who reported similar thickness reduction in their studies. The reduction is explained by  $\text{Co}_3\text{O}_4$  as transitional metal oxide particles will catalyze oxidative degradation of the surface of Kapton during thermal treatment. The change in thickness varied with immersion time which tabulated in Table 1, showing that doping with longer immersion periods leading to a thicker cobalt oxide layer.

**Table 1:** Film thickness of samples.

	Film thickness (mm)			
	Sample 1	Sample 2	Sample 3	Average
Pure Kapton	0.03	0.03	0.03	0.03
30 minutes	0.02	0.02	0.02	0.02
60 minutes	0.03	0.03	0.03	0.03
120 minutes	0.04	0.04	0.04	0.04

#### 4.2. Attenuated Total Reflectance-Fourier Transform Infrared Spectroscopy (ATR-FTIR)

The formation of cobalt oxide on Kapton is confirmed using ATR-FTIR and XRD techniques. Five samples are characterized using ATR-FTIR: pure Kapton, Kapton after KOH treatment (Surface-activated) and Kapton-cobalt oxide composite films formed under varying immersion times (30, 60 and 120 mins). Figure 3 shows the ATR-FTIR result of these five samples.

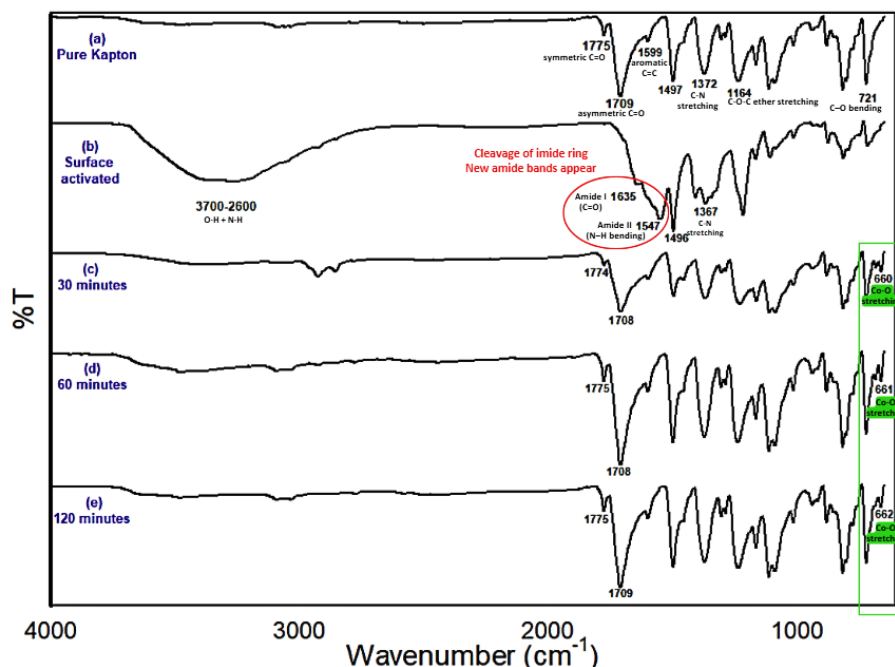


**Figure 3** ATR-FTIR spectrum of (a) Pure Kapton, (b) Surface activated, (c) 30 minutes, (d) 60 minutes and (e) 120 minutes.

ATR-FTIR spectra reveal that pure Kapton exhibited characteristic imide functional group peaks including symmetric and asymmetric C=O stretching, aromatic C=C, C–N, and ether linkages. Upon alkaline treatment with KOH, these peaks disappear and are replaced by bands representing amide and potassium carboxylate groups, confirming surface activation. After thermal treatment at 350 °C, the spectra of the composite films show the reappearance of imide peaks alongside a new peak around 660 cm<sup>-1</sup> corresponding to Co(II)–O bonding, confirming Co<sub>3</sub>O<sub>4</sub> formation (Mu et al., 2010).

#### 4.3. X-Ray Diffraction (XRD)

XRD analysis further supports this. The XRD spectrum in Figure 4 illustrate the structural evolution of Kapton-cobalt oxide composite films after varying immersion times. Pure Kapton showing an amorphous pattern. The most intense peak, the (311) peak will be the key indicator of Co<sub>3</sub>O<sub>4</sub> and expected to appear indeed around 37° (Lakra et al., 2021).

All the composites show emerging crystalline peaks at ~31° and ~37° (2θ), corresponding to the (220) and (311) planes of Co<sub>3</sub>O<sub>4</sub>. These two planes are obvious, surely indicating that Co<sub>3</sub>O<sub>4</sub> crystal is successfully formed in both three conditions (30, 60 and 120 minutes of immersion times). Among the immersion durations, the 30-minute sample exhibits the sharpest and clearest diffraction peaks, indicating more uniform and controlled crystallization compared to the 60- and 120-minute samples, which show signs of structural disorder and over-crystallization respectively.

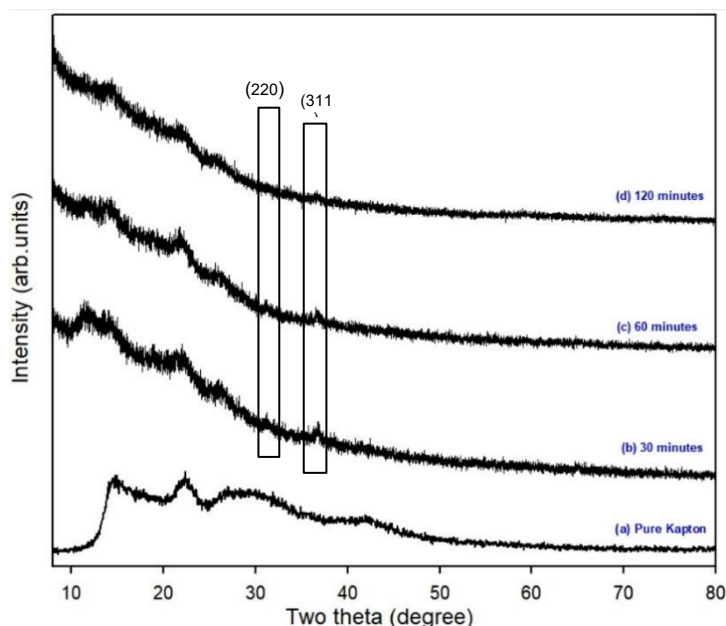


**Figure 4** XRD patterns of (a) Pure Kapton, (b) Surface activated, (c) 30 minutes, (d) 60 minutes and (e) 120 minutes.

#### 4.4. Thermogravimetry Analysis (TGA)

Figure 5 shows the TGA curves of pure Kapton and Kapton-cobalt oxide composite films formed under different immersion times (30, 60, and 120 minutes) in cobalt ion solution. The TGA curves in Figure 5 show that pure Kapton has the highest thermal stability, with  $T_{10}$  occurring at 680 °C, and a 40% weight loss at 850 °C, with a residual mass of 1.80 mg.

In contrast, the Kapton-cobalt oxide composite films exhibit lower thermal stability, with  $T_{10}$  occurring at 480 °C, due to the catalytic effect of  $Co_3O_4$  (Mu et al., 2010). The thermal stability of the composites decreases as the immersion time increases, with weight loss at 850 °C reaching 58% for the 30-minute immersion, 65% for the 60-minute immersion, and 100% for the 120-minute immersion, with corresponding residual masses of 1.26 mg, 1.05 mg, and 0 mg, respectively. The 30-minute immersion sample is the most stable among the composites.

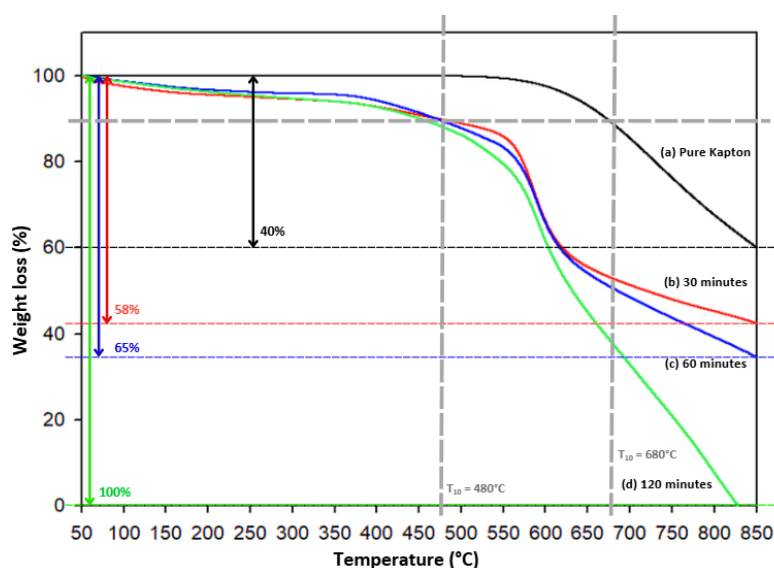


**Figure 5** TGA curves of (a) Pure Kapton, (b) 30 minutes, (c) 60 minutes and (d) 120 minutes.

#### 4.5. Differential Scanning Calorimetry (DSC)

Figure 6 shows the DSC curves of pure Kapton and Kapton-cobalt oxide composite films formed under different immersion times (30, 60, and 120 minutes). The DSC analysis of pure Kapton shows a subtle inflection around 220 °C, indicating its glass transition temperature ( $T_g$ ), which reflects its high thermal stability with no evidence of melting or decomposition.

For the Kapton-cobalt oxide composite films, the  $T_g$  increases with immersion time. The 30-minute composite exhibits a slightly higher  $T_g$  (238 °C), suggesting that the incorporation of cobalt oxide increased the  $T_g$  by reducing polymer chain flexibility. For the 60-minute composite, an endothermic peak at 130 °C is attributed to the evaporation of residual volatiles, possibly due to increased porosity from cobalt oxide. No significant change in  $T_g$  is observed, possibly due to deeper incorporation of cobalt oxide affecting the matrix. The 120-minute immersion shows the highest  $T_g$  (250 °C), indicating that the increased cobalt oxide concentration strengthened the polymer matrix, enhancing its thermal stability and reducing polymer chain mobility (Senthil et al., 2022).

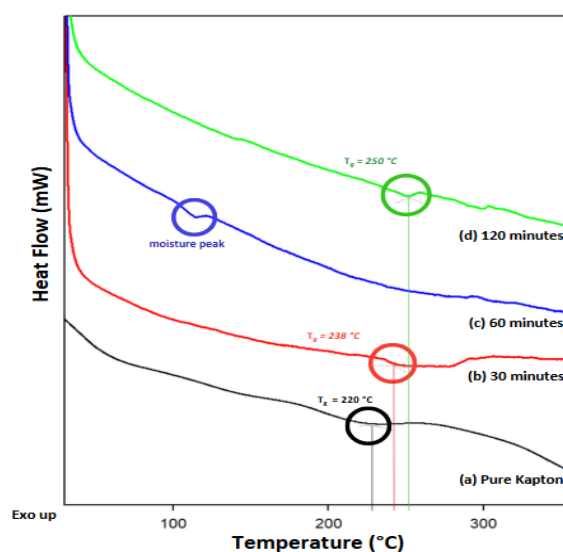


**Figure 6** DSC curves of (a) Pure Kapton, (b) 30 minutes, (c) 60 minutes and (d) 120 minutes.

#### Conclusion

In this study, Kapton-cobalt oxide composite films were successfully prepared using an ion-exchange method with varying immersion times. ATR-FTIR, XRD, TGA, and DSC analyses confirmed the successful incorporation of  $\text{Co}_3\text{O}_4$  into the Kapton matrix, with ATR-FTIR showing a Co-O band at around  $660\text{ cm}^{-1}$  and XRD revealing the best crystallinity for the 30-minute immersion. TGA demonstrated a decrease in thermal stability as compared to pure Kapton due to catalytic effect of  $\text{Co}_3\text{O}_4$  while DSC showed an increase in  $T_g$ , indicating reduced polymer chain flexibility with  $\text{Co}_3\text{O}_4$  integration. Among all samples, the 30-minute immersion is found to be optimal, showing the best crystallinity while maintaining the high thermal stability of Kapton. Overall, the study achieved its objectives in enhancing the functional properties of Kapton without significantly compromising its thermal performance.

#### Acknowledgement

The authors would like to express sincere gratitude to the project supervisor, laboratory staff and all individuals who provided guidance, support and resources throughout the research. Appreciation is also extended to the Faculty of Science, Universiti Teknologi Malaysia for providing access to characterization and thermal analysis facilities.

## References

- Dupont. (2012). DuPont™ Kapton®. [Http://Www.Dupont.Com/Content/Dam/Dupont/Products-and-Services/Membranes-and-Films/Polyimide-Films/Documents/DEC-Kapton-Summary-of-Properties.Pdf](http://www.dupont.com/content/dam/dupont/products-and-services/membranes-and-films/polyimide-films/documents/DEC-Kapton-Summary-of-Properties.Pdf), 50, 1–7.
- Jacobs, I. E., Lin, Y., Huang, Y., Ren, X., Simatos, D., Chen, C., Tjhe, D., Statz, M., Lai, L., Finn, P. A., Neal, W. G., D'Avino, G., Lemaur, V., Fratini, S., Beljonne, D., Strzalka, J., Nielsen, C. B., Barlow, S., Marder, S. R., ... Sirringhaus, H. (2022). High-Efficiency Ion-Exchange Doping of Conducting Polymers. *Advanced Materials*, 34(22). <https://doi.org/10.1002/adma.202102988>
- Kim, J. M., Zhang, X., Zhang, J. G., Manthiram, A., Meng, Y. S., & Xu, W. (2021). A review on the stability and surface modification of layered transition-metal oxide cathodes. *Materials Today*, 46(xx), 155–182. <https://doi.org/10.1016/j.matod.2020.12.017>
- Lakra, R., Kumar, R., Nath Thatoi, D., Kumar Sahoo, P., & Soam, A. (2021). Synthesis and characterization of cobalt oxide (Co<sub>3</sub>O<sub>4</sub>) nanoparticles. *Materials Today: Proceedings*, 41(xxxx), 269–271. <https://doi.org/10.1016/j.matpr.2020.09.099>
- Miranda-López, M. I., Padilla-Zarate, E. A., Hernández, M. B., Falcón-Franco, L. A., García-Villarreal, S., García-Quiñonez, L. V., Zambrano-Robledo, P., Toxqui-Terán, A., & Aguilar-Martínez, J. A. (2020). Comparison between the use of Co<sub>3</sub>O<sub>4</sub> or CoO on microstructure and electrical properties in a varistor system based on SnO<sub>2</sub>. *Journal of Alloys and Compounds*, 824. <https://doi.org/10.1016/j.jallcom.2020.153952>
- Mu, S., Wu, Z., Wang, Y., Qi, S., Yang, X., & Wu, D. (2010). Formation and characterization of cobalt oxide layers on polyimide films via surface modification and ion-exchange technique. *Thin Solid Films*, 518(15), 4175–4182. <https://doi.org/10.1016/j.tsf.2009.12.004>
- Ratnayake, S. P., Ren, J., Colusso, E., Guglielmi, M., Martucci, A., & Della Gaspera, E. (2021). SILAR Deposition of Metal Oxide Nanostructured Films. *Small*, 17(49). <https://doi.org/10.1002/sml.202101666>
- Senthil, T., Vasanthi, P., Chandramohan, A., Prabukanthan, P., & Dinakaran, K. (2022). Synthesis and characterization of manganese doped cobalt oxide porous nanoparticles dispersed epoxy composites. *Materials Today: Proceedings*, 59, 1022–1027. <https://doi.org/10.1016/j.matpr.2022.02.281>